applied sciences

MDPI

Article

Structural Response of Double-Layer Steel Cylinders under Inside-Explosion Loading

Xuejun Qin, Jun Yang, Junyi Guan, Zhen Liao, Yanjun Ma and Dezhi Zhang *

Northwest Institute of Nuclear Technology, Xi'an 710024, China
* Correspondence: zhangdzf@163.com

Abstract: The research on the structural response of explosive vessel is an important basis for the design of explosive vessels. Double-layer cylinder structures are widely used in the design of various explosive vessels. This paper studied the deformation of a steel cylindrical shell under internal explosion and proposes a new method for measuring shell deformation by PDV (photonic Doppler velocimetry). We carried out many spherical explosive experiments and obtained useful results that show displacement of the double-layer cylinders and the explosion time. The above process is a simulated LS-DYNA with a finite element numerical simulation. The vibration period of the outer cylindrical shell and the time for reflection of the stress wave in the outer cylindrical shell were obtained by numerical simulation and PDV measurement, respectively. The results of both can be verified against each other. Through the above research, the structural response of the multilayer cylinders can be obtained, which can provide further help with research of the structural design of multilayer cylinders.

Keywords: inside-explosion; double-layer steel cylindrical shells; PDV (photonic Doppler velocimetry); deformation; numerical simulation

check for updates

Citation: Qin, X.; Yang, J.; Guan, J.; Liao, Z.; Ma, Y.; Zhang, D. Structural Response of Double-Layer Steel Cylinders under Inside-Explosion Loading. *Appl. Sci.* **2023**, *13*, 709. https://doi.org/10.3390/app13020709

Academic Editor: Lina M. López

Received: 10 December 2022
Revised: 24 December 2022
Accepted: 29 December 2022
Published: 4 January 2023

Copyright: © 2023 by the authors. Licensee MDPI, Basel, Switzerland. This article is an open access article distributed under the terms and conditions of the Creative Commons Attribution (CC BY) license (https://creativecommons.org/licenses/by/4.0/).

1. Introduction

Explosive vessels are important as safety protection equipment for national defense and industrial application, and the research on the structural response of explosive vessels is an important basis for their design. The dynamic deformation characteristics of steel cylindrical shells under internal explosion have theoretical significance as well as applied value, and many scholars have studied the deformation of steel cylinders under the action of internal explosions. Duffy studied the strain hardening and strain rate sensitivity of an elastic–plastic steel cylinder [1]. Based on experimental and numerical simulation methods, Fangping Zhong and Yunxiao Cui studied the plastic deformation of a multilayer cylindrical steel cylinder subjected to explosions with spherical and cylindrical charges [2,3]. The deformation and failure characteristics of a steel cylinder under internal explosion were researched through experimental and numerical simulations [4–6]. Y. Du et al. researched and proposed a coupled finite element method—smooth particle hydrodynamics (FEM-SPH) approach to simulate the fracture of a cylindrical shell subjected to internal explosion [7]. V. A. Ryzhanskii et al. studied a steel cylindrical shell filled with water or air under internal explosion [8]. Jianyuan Wu et al. conducted a study on the dynamic response of a metal cylindrical shell under the combined effects of fragments and shock waves through experimental and numerical investigations [9]. McDonald et al. researched the experimental response of four modern steels by localized blast loading [10]. Kai Zheng et al. studied the mechanical behavior of a composite steel structure under explosion load through experiment and simulation [11]. Caiyu Yin et al. analyzed the shock mitigation effects of sacrificial coatings plastered onto stiffened double cylindrical shells via simulation [12]. Shizhang Huang et al. researched the behaviors of double cylindrical shells subjected to an underwater explosion [13]. Jianguo Ning et al. proposed a three-dimensional (3D)

embedded Eulerian–Lagrangian method to simulate the 3D fluid-structure interaction (FSI) problems subjected to an explosion and impact loading [14]. Nassiraei, H. investigated the local joint flexibility (LJF) of tubular K-joints reinforced with external plates, and a finite element (FE) model was generated and verified with the results of several available experimental tests and equations [15]. Pham Van Vinh et al. studied a plate element for the static bending analysis of functionally graded plates based on a higher-order shear deformation theory [16,17]. Cheng Zheng et al. studied the dynamic response of steel plates under blast loading by experimental and numerical simulation [18]. Shujian Yao et al. investigated the dynamic response of a steel box girder under internal blast loading through experiments and numerical simulation [19]. Shiqi Fu et al. proposed reasonable scaling coefficients to the scale model experiment of a cylindrical lattice shell under internal explosion [20]. Haiteng Wang et al. used the AUTODYN and LS-DYNA software to study the influencing factors of anti-explosion performance of a steel structure's protective doors under chemical explosion conditions [21]. R. Rajendran et al. evaluated the performance of an HSLA steel underwater explosion [22]. The deformation experiment and numerical simulation of a steel cylinder structure under internal explosion is of great significance for analyzing and studying the response of a steel cylinder structure.

There are many different ways to measure shell deformation. For example, Fangping Zhong attached strain gauges to the outer wall of a metal cylinder to measure the dynamic deformation of the vessels [23]. Tiegang Tang used a high-speed camera to take continuous pictures of the deformation of the metal cylinder under the blast load in order to obtain the deformation of the metal cylinder [24]. Yongle Hu used the Doppler effect of lasers to measure the radial deformation of explosive containers [25]. Jin Li measured the large strain over 20% of a steel cylinder with strain wire technology [26]. Xuejun Qin measured the radial displacement of a single-layer steel cylinder by using an electrical probe technique [27]. These testing methods are now mainly used to measure the outer wall of a single-layer steel cylinder. There are no relevant reports about taking simultaneous measurements of the relationship between deformation and explosion time for double-layer steel cylindrical shells.

In this paper, the inner and outer wall radial motion of double-layer steel cylindrical shells under internal 120 gTNT yield explosion are studied by PDV based on the laser Doppler effect and numerical simulation. This research of the deformation of inner and outer cylinders is used to study the structural response of double-layer steel cylindrical shells.

2. PDV Measurement System

The technical principle of PDV for measuring the deformation of double-layer steel cylinders under internal explosions is based on the laser Doppler effect, which is an optical test method that can measure the displacement of an object by combining laser technology and interferometric technology. The principle of PDV measurement is that an incident laser shines on a moving particle and the scattering laser produces a Doppler frequency shift, as is shown in Figure 1. Its advantages include the characteristics of non-contact, higher accuracy, faster dynamic response, and larger measurement range [28].

Compared with contact measurement, PDV measurement has a smaller focused light spot with other methods, which can be considered to reflect the motion of the point, and non-contact measurement does not affect the structure of the double-layer steel cylinders, suffers less interference from electromagnetic pulse, has very high displacement resolution and fast response, and can meet the requirements of measuring the high speed and large deformation dynamic process of the double-layer steel cylinders.

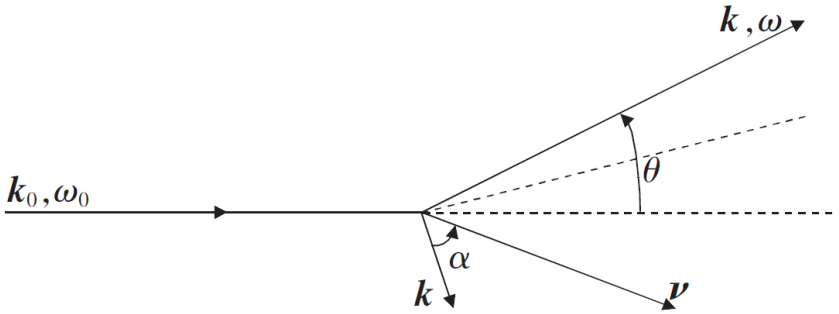


Figure 1. Laser Doppler frequency shift caused by moving object (Where k_0 is incident light vector, k is scattering light vector, v is particle velocity vector, ω_0 is the frequency of incident light, ω is the frequency of scattered light, and θ is the phase).

In the process of studying the motion law of an object under explosion load, an optical fiber probe is generally used to perform the function of transmitting and receiving the laser. As is shown in Figure 1, $\theta = 180°$, the laser Doppler frequency shift scalar formula can be obtained when the object is away from the probe.

$$\Delta f(t) = 2\frac{v(t)}{\lambda_0} \tag{1}$$

where $\Delta f(t)$ is the frequency shift scalar, λ_0 is the laser wavelength in vacuum, $v(t)$ is the velocity of object movement, and the velocity is positive when the object moves close to the probe. On the contrary, the velocity is a negative value.

There is a certain gap between the inner steel cylinder and the outer steel cylinder of double-layer shells. A small hole is opened in the outer steel cylinder facing the burst core, to measure the displacement of the inner steel cylinder by PDV. Another PDV is used to measure the displacement of the outer steel cylinder facing the blast core. After the detonation of the spherical explosive, the shock wave loads onto the inner wall of the inner steel cylinder, causing deformation of the inner steel cylinder, and the deformation information of the outer wall of the inner steel cylinder is recorded to the oscilloscope through the PDV measurement system. When the inner steel cylinder comes into contact with the outer steel cylinder, it causes deformation of the outer steel cylinder. After the deformation information of the outer steel cylinder is recorded to the oscilloscope through another PDV measurement system, deformation of the inner steel cylinder and the outer steel cylinder at different moments can be obtained. The deformation of the double-layer steel cylinders measured by the PDV system is shown in Figure 2.

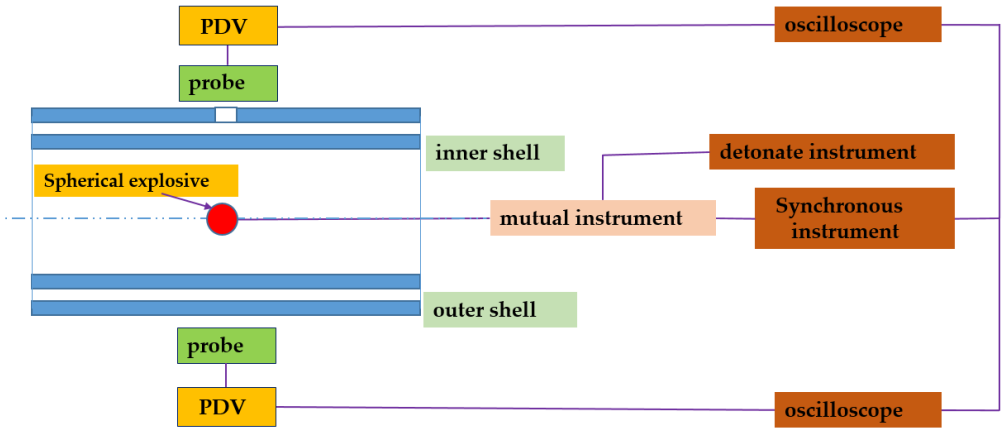


Figure 2. Schematic diagram of PDV measurement system.

3. Experimental Scheme

The material of the double-layer steel shells used in the experiment is steel-20, the chemical compositions of steel-20 includes 0.24% C, 0.27% Si, 0.52% Mn, 0.035% S, 0.035% P, 0.25% Cr, 0.25% Ni, and 0.25% Cu. The yield strength and tensile strength are 245 and 410 MPa, respectively. The weight of double-layer steel shells is equivalent to an single-layer steel shell, which is 600 mm length, 100 mm inner diameter and 12 mm thickness, in order to study the blast resistance performance of double-layer steel shells under the same explosive yield. The parameters of the double-layer steel shells are shown in Table 1.

Table 1. Parameters of double-layer steel shells.

Number	*L*/mm	*R*/mm	h_1/mm	Δ/mm	h_2/mm
No. 1	600	50	4	4	7.5
No. 2	600	50	6	4	5.6
No. 3	600	50	8	4	3.8

Where L is the length of the double-layer steel cylinders, R is the internal radius of the double-layer steel cylinders, h_1 is the thickness of the inner steel cylinder, Δ is the gap between the inner steel cylinder and the outer steel cylinder, and h_2 is the thickness of the outer steel cylinder.

The spherical explosive is composed of RDX/TNT (60/40), which equals 120 gTNT, and the center detonation mode is adopted. Figure 3 shows that the explosive is installed in the center of the double-layer steel cylinders through a cross made of organic glass of 1.5 mm thickness, which ensures positioning accuracy and reduces the influence of explosive load. The minimum distance from the double-layer cylinder to the center of the explosion is 0.05 m, and the explosion yield is 120 gTNT; thus, the minimum scaled distance is 0.1 m/kg$^{1/3}$.

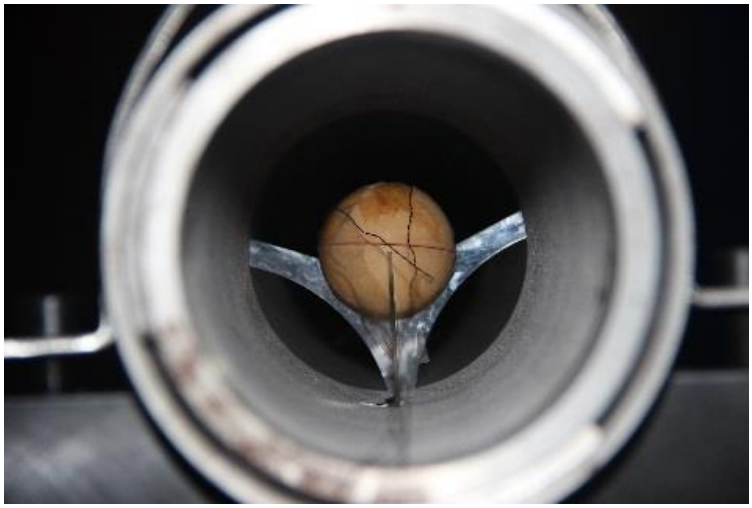


Figure 3. Installation of spherical charge in the double-layer cylindrical shells.

By opening a small through-hole of ϕ 3 mm in the outer steel cylinder in the direction of the explosion center, a PDV probe can be set to measure the deformation of the inner steel cylinder through the hole, while another PDV probe is set to measure the deformation of the outer steel cylinder. The experimental device for measuring the deformation of the double-layer steel shells by the PDV system is shown in Figure 4.

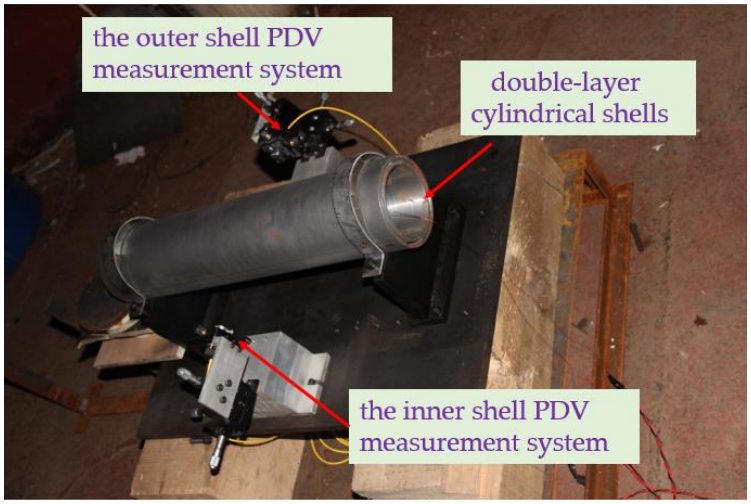


Figure 4. Experimental device of PDV measurement double-layer cylindrical shells.

4. Analysis of Experimental Results

4.1. Results of PDV Measurement

The relationship between the time and the deformation of the double-layer steel cylindrical shells under a 120 gTNT explosion was obtained by PDV measurement, and the velocity curves of the inner and outer cylinders are shown in Figure 5. It can be found that the maximum velocity of the inner cylinder is 151.2 m/s. After the collision of the inner and outer cylinders, some part of the outer wall of the inner cylinder was embedded into the ϕ 3 mm through-hole of the outer cylinder, causing an instant increase in inner cylinder velocity, which led to a peak in the curve. After the collision, the velocity of the inner cylinder decreased while the velocity of the outer cylinder increased to the maximum value of 85.6 m/s. It can be seen that it takes 35.7 μs for the outer wall of the inner shell from the start of deformation to contact the inner wall of the outer shell. The gap between the inner shell and outer shell is 4 mm, and the average velocity of the radial movement of inner shell before the impact of the outer shell was calculated to be about 112 m/s.

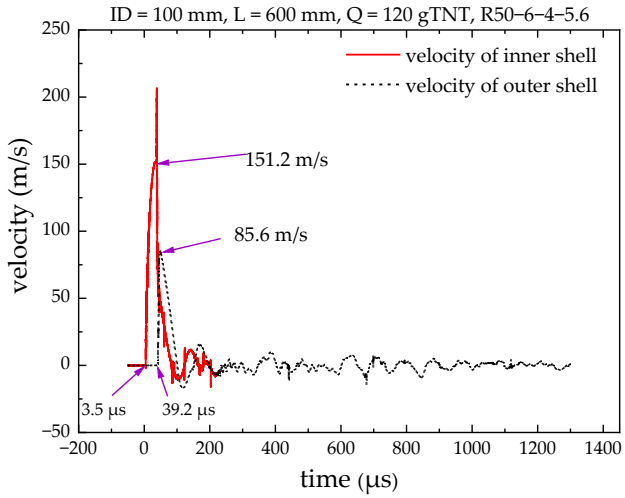


Figure 5. Velocity of double-layer shells measured by PDV.

As is shown in Figure 6, the relationship between radial displacement and time of the inner cylinder and outer steel cylinder measured by PDV can be obtained by integrating the curves of the velocities. The maximum radial displacement of the inner cylinder is 5.41 mm and that of the outer cylinder is 2.45 mm.

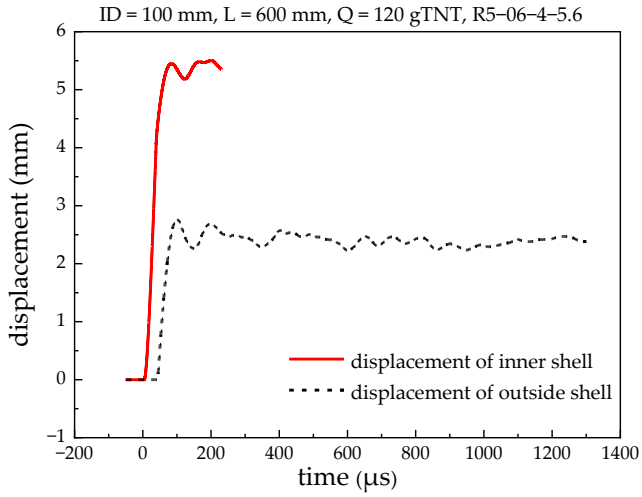


Figure 6. Displacement of double-layer shells measured by PDV.

The maximum radial displacement of the outer cylinder was measured to be 2.54 mm after the experiment, compared to which the error of PDV measurement was about 2.8%. After incising the double-layer cylinder, the maximum radial displacement of the inner cylinder was measured to be 5.72 mm after the experiment, compared to which the error of PDV measurement was about 5.4%. It can be concluded that the radial displacement measured by PDV was in accordance with that measured after the experiment.

The maximum velocities of the three double-layer cylindrical shells under 120 gTNT explosive yield were measured by PDV. The maximum velocities of the three experiments are shown in Table 2. The maximum velocities of the inner shell are reduced with the increase in the thickness of the inner cylindrical shell. The maximum velocities of the outer shell increase at first and then decrease with the increase in the thickness of the inner shell.

Table 2. The maximum velocities of the inner and outer shells.

Number	h_1/mm	Δ/mm	h_2/mm	Maximum Velocity of the Inner Shell (m/s)	Maximum Velocity of the Outer Shell (m/s)
No. 1	4	4	7.5	201.4	82.3
No. 2	6	4	5.6	151.2	85.6
No. 3	8	4	3.8	100.6	62.2

4.2. Deformation of the Double-Layer Cylindrical Shells

To measure the deformation of the inner cylindrical shell after the experiment, the double-layer steel cylindrical shells need to be linearly cut, as shown in Figure 7. It is obvious that the inner cylindrical shell is not deformed by the cutting. As a result, it is considered that the measurement results of the deformation will not be affected by cutting.

The results comparing the deformation of the outer cylinder in the three experiments with the single-layer cylinder of 12 mm thickness at the same burst yield are shown in Figure 8.

The following two conclusions can be obtained from Figure 8: (1) When the gap is constant, with the increase in the thickness of the inner shell, the deformation range of the outer wall of the double-layer shell is significantly smaller than the 12 mm thickness single-layer shell, which is in the range of ± 1R. (2) When the gap of the double-layer shells is constant, the deformation of the single-layer cylinder is smaller than the double-layer shells in a certain range, which indicates that the anti-burst performance of single-layer shell is better than the double-layer shells. The deformation of the double-layer shells becomes smaller than the single-layer shell, and the thickness of the inner cylinder increases,

indicating that the anti-burst performance of the double-layer cylinders is better than the single-layer cylinder.

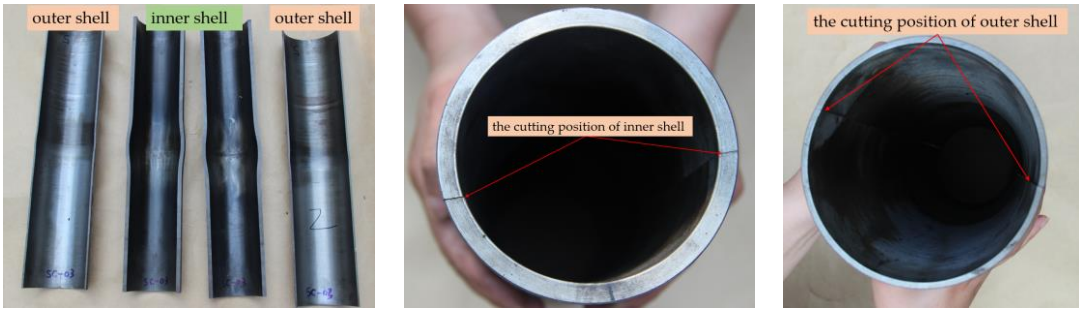


Figure 7. Photographs of double-layer steel cylinders after cutting. (**a**) Double-layer shells after cutting. (**b**) Inner shell after cutting. (**c**) Outer shell after cutting.

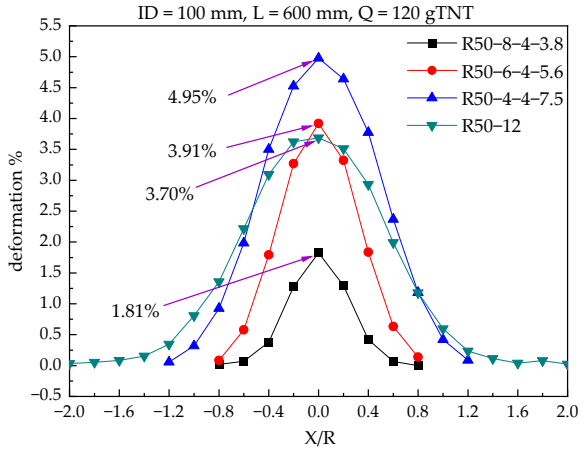


Figure 8. Comparison of the deformation of a single shell to double-layer shells.

The following two conclusions can be obtained from Figure 9: (1) The increase in the thickness of the inner shell results in a gradual decrease in the maximum deformation of the inner shell, and the deformation of the inner shell tends to be stable after the thickness of the inner shell reaches a certain value, the limiting case of which is the single-layer shell. (2) The deformation range of the inner shell is ± 1.4R, which is significantly larger than the outer shell.

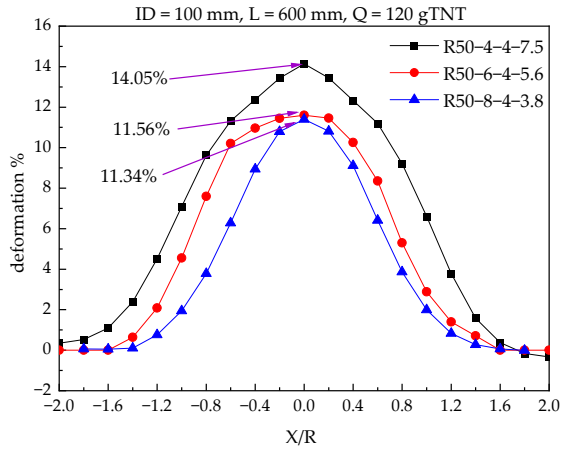


Figure 9. Inner shell deformation of double-layer shells.

5. The Numerical Simulation of Double-Layer Cylindrical Shells

5.1. The Model of Numerical Simulation

A numerical simulation of the deformation process of double-layer steel shells through the LS-DYNA program was conducted to show the deformation of the inner shell and outer shell changing with time under an internal explosion [29]. As is shown in Figure 10, a two-dimensional axisymmetric model is used: ① and ② are symmetry boundaries, and ③ and ④ are outflow boundaries. The air filled inside the inner shell and between the double-layer shells is set as an ideal gas. An Euler grid is used for the explosion and air while a Lagrange grid is used for steel shells, and the flow-solid coupling algorithm is defined between the two types of grids, which can transfer the interaction.

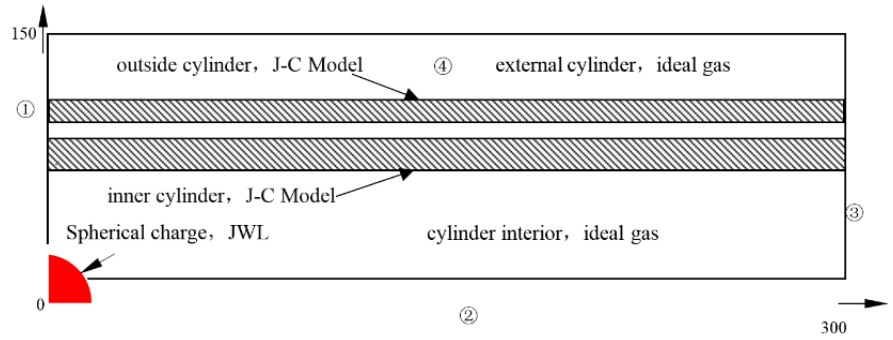


Figure 10. Two-dimensional axisymmetric model of double-layer cylinders.

5.2. The Equation of Numerical Simulation

Equation (2) is the ideal gas equation of state for air [30], where the adiabatic index γ = 1.4, initial density ρ_0 = 1.225 kg/m^3, initial specific internal energy e_0 = 206.8 kJ/kg, and initial air pressure P_0 = 101.332 kPa.

$$P = (\gamma - 1)\rho e_0 \tag{2}$$

The standard JWL equation of state is used for the explosion products in Equation (3) [31,32].

$$p = A_0(1 - \frac{\omega}{R_1\overline{v}})e^{-R_1\overline{v}} + B_0(1 - \frac{\omega}{R_2\overline{v}})e^{-R_2\overline{v}} + \frac{\omega^* e\rho_{00}}{\overline{v}} \tag{3}$$

where $\overline{v}$ is the specific volume, A_0, B_0, R_1, R_2, ω^* are all the related parameters of the explosion, the initial density of explosion ρ_{00} is 1.63 g/cm^3, the C-J blast wave velocity is 6930 m/s, and the initial energy is 6 × 10^9 J/m^3.

The Johnson–Cook strength model is used for the double-layer steel shells in Equation (4).

$$\sigma = (A + B\varepsilon^n)\left(1 + C\ln\dot{\varepsilon}^*\right) \tag{4}$$

where A, B, n, C are the material constants, A is the yield strength at the strain rate of 1 s^{-1}, B is the strain-hardening coefficient, n is the strain-hardening index, C is the strain rate correlation index, and ε* is the reference strain ratio. Table 3 is the material parameters.

Table 3. Material parameters.

Johnson-Cook Model	***A*/MPa**	**B/ MPa**	***n***	***c***	**Reference Strain Rate/s^{-1}**
	370	700	0.4	0.055	1.0
JWL equation of state	**A_0/GPa**	**B_0/GPa**	**ω^***	**R_1**	**R_2**
	374	3.74	0.35	4.15	0.9

5.3. Results of Numerical Simulation

5.3.1. Shock Wave Pressure in the Double-Layer Shells

The pressure data observation points are set at 50 mm intervals along the inner steel cylinder, and the observation points numbers are from T1 to T6, as shown in Figure 11. Figure 12 shows the extracted overpressure time curve of each observation point; the maximum overpressure is 641.9 MPa at 11.8 μs.

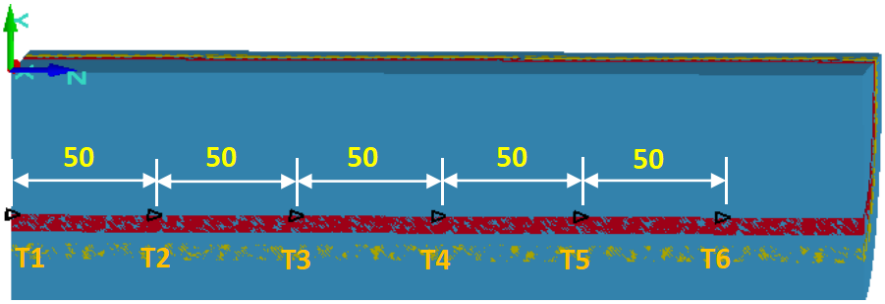


Figure 11. The pressure data observation points.

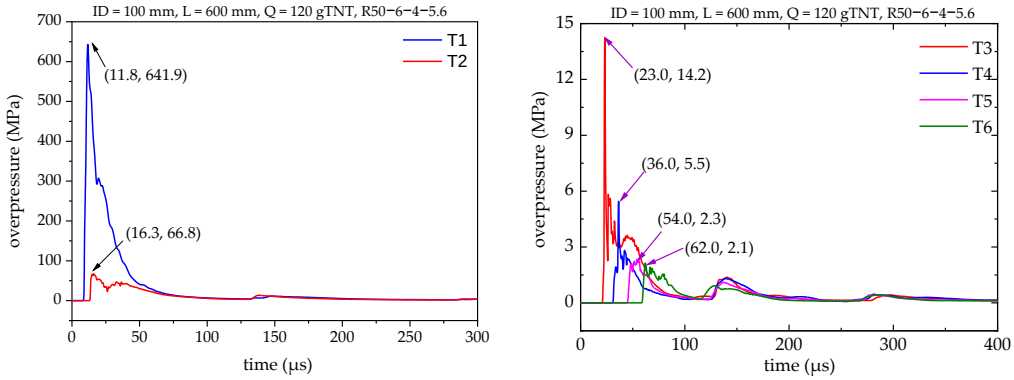


Figure 12. The overpressure curves of T1 to T6.

5.3.2. Analysis of Collision Process of the Inner and Outer Steel Shells

In the numerical simulation of the No. 2 experiment, when the shock wave acts on the inner steel shell, the inner shell deforms along the circumferential direction, and then, the inner shell collides with the outer steel shell, as is shown in Figure 13.

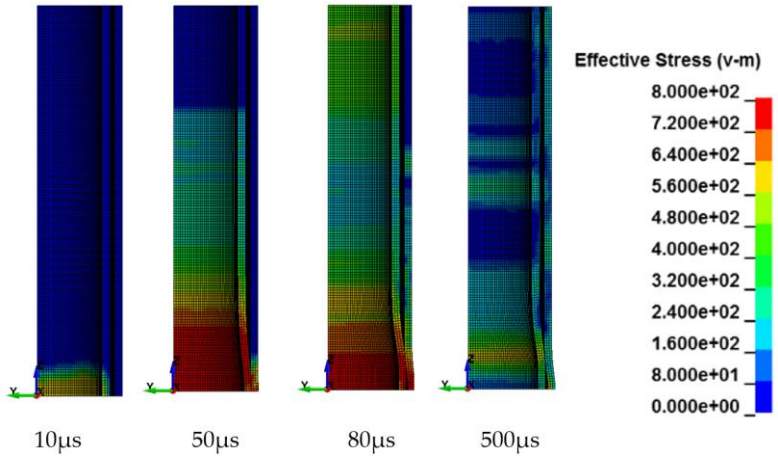


Figure 13. Stress distribution cloud of double-layer steel shells.

Figure 14 shows the process of the interaction between the inner shell and the outer shell at different times. The inner shell begins to collide with the outer shell at 45 μs, the first separation time of the inner steel shell and outer steel shell is about 110 μs, the second collision of the inner shell and the outer shell occurs at 145 μs, the second separation time of the inner steel shell and outer steel shell is about 180 μs, the third collision of the inner shell and outer shell occurs at 220 μs, and the third separation time of the inner steel shell and outer steel shell is about 260 μs.

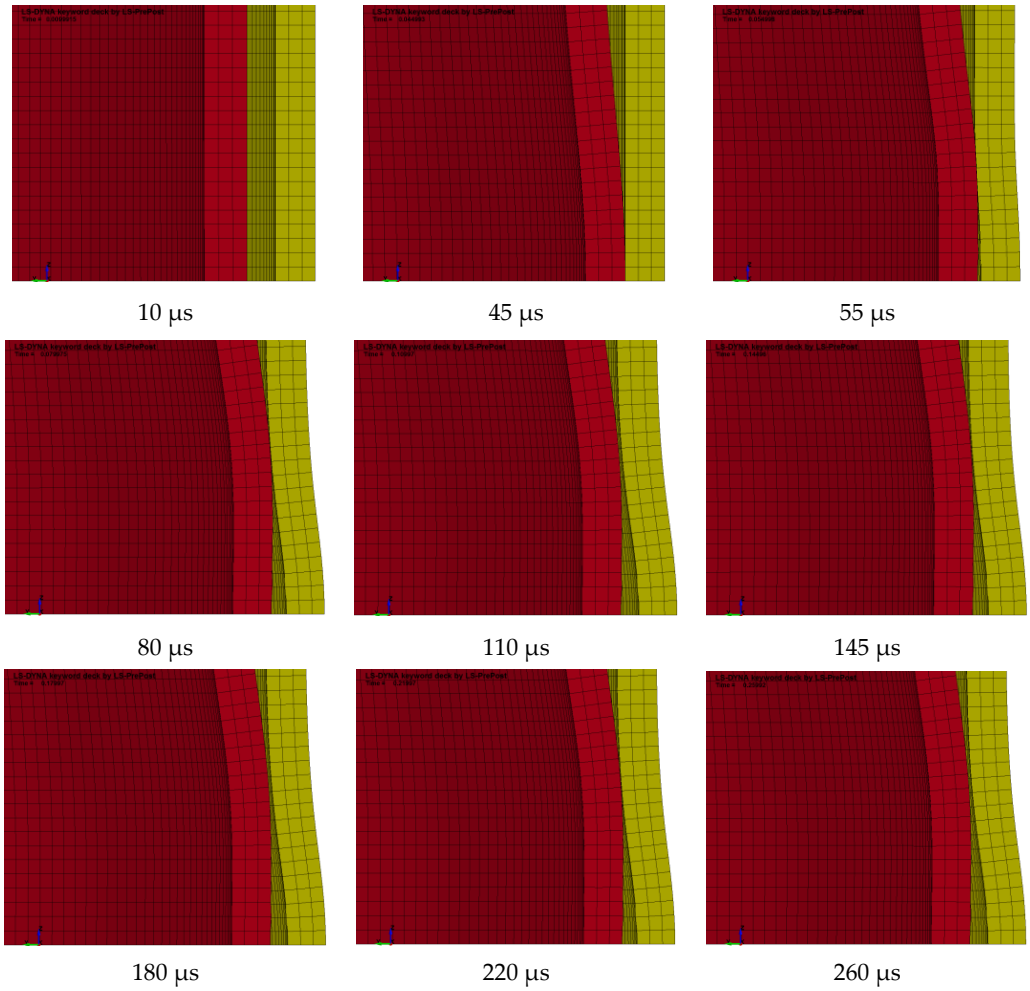


Figure 14. Collision process of double-layer steel cylindrical shells.

5.3.3. The Velocities of Double-Layer Cylindrical Shells by Simulation

The radial velocity curves of the double-layer steel cylinders given by numerical simulation and PDV measurement are shown in Figure 15, which are basically matched. The maximum velocity of the inner cylinder given by the simulation is 150.8 m/s, while the velocity measured by PDV is 151.2 m/s, with an error of 0.2%. The maximum velocity of the outer cylinder given by the simulation is 121.1 m/s, while the velocity measured by PDV is 85.6 m/s, with an error of 41.5%. The larger error is caused by the vibration of the PDV measuring devices during the explosion.

The radial displacement curves of the double-layer steel cylinders given by numerical simulation and PDV measurements are shown in Figure 16, which are basically matched. The maximum displacement of the inner cylinder given by simulation is 5.29 mm, while that measured by PDV is 5.41 mm, with an error of 2.2%. The maximum displacement of the outer cylinder given by the simulation is 2.67 mm, while that measured by PDV is 2.45 mm, with an error of 8.2%. It can be concluded that the results shown by the numerical simulation and PDV measurement are coincidental.

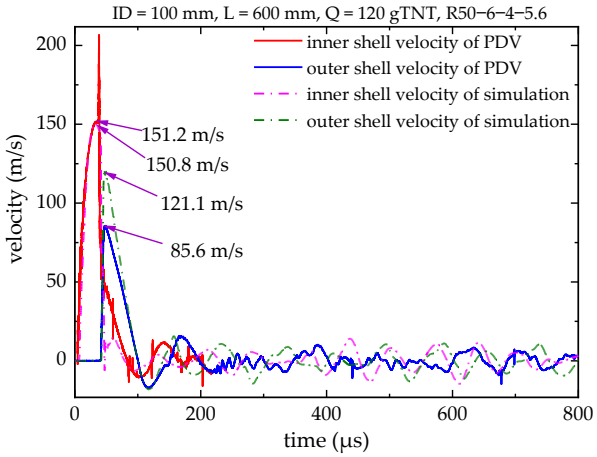


Figure 15. Velocity comparison of PDV measurement and simulation.

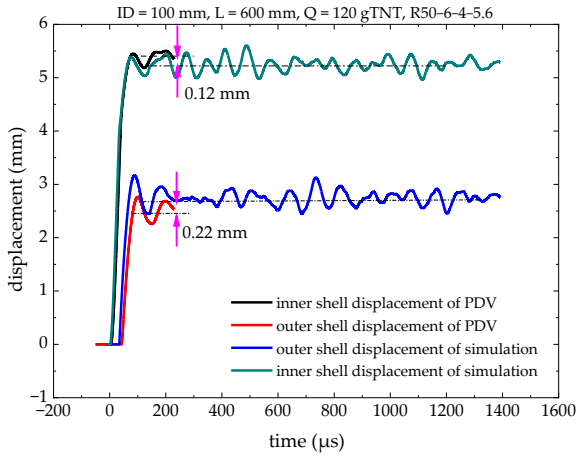


Figure 16. Displacement comparison of PDV measurement and simulation.

The velocity curves of the outer cylinder obtained by numerical simulation and PDV measurement in experiment No. 3, using double-layer steel cylindrical shells of 100 mm inner diameter, 8 mm thickness of the inner cylindrical shell, 3.8 mm thickness of the outer cylindrical shell and 4 mm gap between the inner shell and the outer shell, are shown in Figure 17. Figure 18 shows an enlarged figure of the front part of the above two curves.

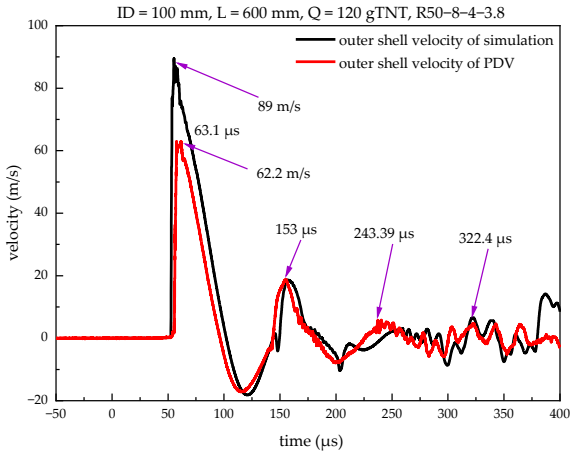


Figure 17. Velocities of PDV measurement and simulation.

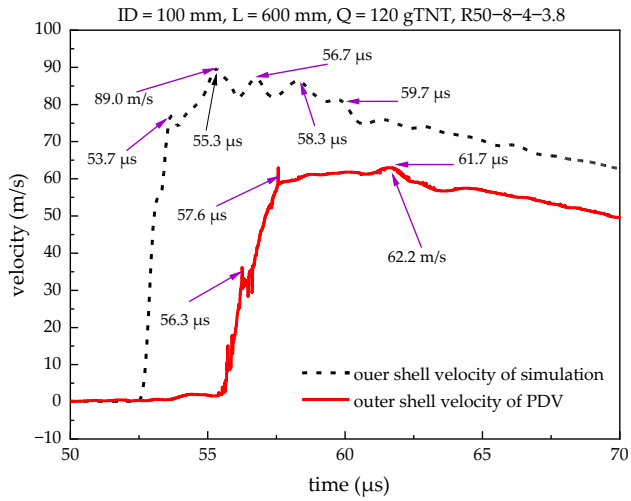


Figure 18. Magnification of the front velocity waveform.

The period of vibration of the outer steel shell is given by the theoretical calculation as follows, in which C_0 is the velocity that the stress wave propagates in the steel.

$$\Delta T_1 = \frac{2\pi(R + h_1 + \Delta + \frac{h_2}{2})}{C_0} = \frac{2 \times 3.14 \times 0.0639}{5000} = 80.3\ \mu s$$

According to the stress wave theory, the time for the stress wave to finish a back-and-forth reflection in the outer shell is given below.

$$\Delta T_2 = \frac{2h_2}{C_0} = \frac{2 \times 0.0038}{5000} = 1.52\ \mu s$$

Forced vibration happened to the outer cylindrical shell in the first 1/4th period, and then, the vibration period was 90 μs, which was slightly greater than the conclusion of the theoretical analysis. The results of time for a back-and-forth reflection of the stress wave in the outer cylinder given by numerical simulation and PDV measurement are in accordance with the theoretical analysis.

6. Conclusions

By measuring the deformation of the double-layered steel cylindrical shells under the internal explosion through PDV, and by comparing it with the results obtained from the numerical simulation and post-experimental measurements, the conclusions are as follows.

(1) This paper proposed a new method for measuring the deformation of double-layer steel cylindrical shells under internal explosion by PDV; the results of the deformation of the inner and outer cylindrical shells by PDV and numerical simulation are basically matched. Comparing the post-experimental results of the deformation of the double-layer shells with the results of the PDV and numerical simulations, it can be found that the error of maximum deformation is less than 10%.

(2) The vibration period of the outer cylindrical shell and the time for reflection of the stress wave in the outer shell given by the numerical simulation and PDV measurement are consistent.

(3) When the gap between the double-layer cylinders is constant, the deformation range of the outer cylinder is ± 1R, which is significantly smaller than the single-layer cylinder with an increase in the thickness of the inner cylinder, while the deformation range of the inner cylinder, which is in the range ± 1.4R, is significantly greater than the outer cylinder.

(4) When the thickness of the inner layer increases, the maximum deformation of the inner cylinder gradually decreases. It can be seen from the trend of the deformation

of the inner shell that the inner thickness has increased to a certain value of which the limiting case is a single-layer cylinder.

Based on the method of PDV and the numerical simulations used to study the structural response of the double-layer cylindrical shells, the deformation history of each layer of a multi-layer steel cylindrical shell under internal explosion can be researched, and the structure design of multi-layer steel cylindrical shells can be further optimized.

Author Contributions: X.Q., J.Y. and D.Z. conceived and designed the experiments; X.Q., J.Y., Y.M. and J.G. performed the experiments; X.Q. and Z.L. carried out the numerical simulations and analyzed the data; X.Q. wrote the paper. All authors have read and agreed to the published version of the manuscript.

Funding: This research received no external funding.

Institutional Review Board Statement: Not applicable.

Informed Consent Statement: Not applicable.

Data Availability Statement: All data included in this study are available upon request by contacting the corresponding author.

Conflicts of Interest: The authors declare no conflict of interest.

Abbreviations

Symbol List

k_0	incident light vector;
k	scattering light vector;
v	particle velocity vector, m/s;
ω_0	frequency of incident light, Hz;
ω	frequency of scattered light, Hz;
θ	phase;
λ_0	laser wavelength in vacuum, nm;
$v(t)$	velocity of object movement, m/s;
Q	explosive yield, gTNT;
L	length of double-layer steel cylinders, mm;
R	internal radius of double-layer steel cylinders, mm;
h_1	thickness of inner steel cylinder, mm;
Δ	gap between inner steel cylinder and outer steel cylinder, mm;
h_2	thickness of outer steel cylinder, mm;
γ	adiabatic index;
ρ_0	the ideal gas initial density, kg/m^3;
e_0	initial specific internal energy, kJ/kg;
P_0	initial air pressure, kPa;
$\overline{v}$	specific volume;
ρ_{00}	initial density of explosion, kg/m^3;
A_0	parameter of explosion, GPa;
B_0	parameter of explosion, GPa;
R_1	parameter of explosion;
R_2	parameter of explosion;
ω^*	parameter of explosion;
A	steel shell yield strength at strain rate of 1 s^{-1}, MPa;
B	steel shell strain hardening coefficient, MPa;
n	steel shell strain hardening index;
C	steel shell strain rate correlation index;
ε^*	reference strain ratio;
C_0	velocity that stress wave propagates in steel, m/s.
ID	Internal Diameter

References

1. Duffey, T.; Krieg, R. The effects of strain-hardening and strain-rate sensitivity on the transient response of elastic-plastic rings and cylinders. *Int. J. Mech. Sci.* **1969**, *11*, 825–844. [CrossRef]
2. Zhong, F.P.; Ma, Y.J.; Zhang, D.Z. Research on plastic deformation of multi-layer cylindrical steel tube subjected to blasts of spherical and cylindrical charges. *Acta Armamentarii* **2009**, *30*, 194–196.
3. Cui, Y.X.; Hu, Y.L.; Wang, C.M. Dynamic response of multi-layer steel cylinder under internal intense blast loading. *Explos. Shock Waves* **2015**, *35*, 820–824.
4. Wang, D.; Qin, X.; Chen, W.; Wang, S. Simulation of the Deformation and Failure Characteristics of a Cylinder Shell under Internal Explosion. *Appl. Sci.* **2022**, *12*, 1217. [CrossRef]
5. Malekan, M.; Khosravi, A.; Cimini, C.A. Deformation and fracture of cylindrical tubes under detonation loading: A review of numerical and experimental analyses. *Int. J. Press. Vessel. Pip.* **2019**, *173*, 114–132. [CrossRef]
6. Hiroe, T.; Fujiwara, K.; Hata, H.; Takahashi, H. Deformation and fragmentation behavior of exploded metal cylinders and the effects of wall materials, configuration, explosive energy and initiated locations. *Int. J. Impact Eng.* **2008**, *35*, 1578–1586. [CrossRef]
7. Du, Y.; Ma, L.; Zheng, J. Fracture of Cylindrical Shells Subjected to Internal Explosion: Numerical Simulation. *Procedia Eng.* **2015**, *130*, 1695–1704. [CrossRef]
8. Ryzhanskii, V.A.; Syrunin, M.A. Explosion resistance of a steel cylindrical shell. *Combust. Explos. Shock Waves* **2011**, *47*, 115–122. [CrossRef]
9. Wu, J.; Ji, C.; Long, Y.; Song, K.; Liu, Q. Dynamic responses and damage of cylindrical shells under the combined effects of fragments and shock waves. *Thin-Walled Struct.* **2017**, *113*, 94–103. [CrossRef]
10. McDonald, B.; Bornstein, H.; Langdon, G.; Curry, R.; Daliri, A.; Orifici, A. Experimental response of high strength steels to localised blast loading. *Int. J. Impact Eng.* **2018**, *115*, 106–119. [CrossRef]
11. Zheng, K.; Xu, X. Experimental and Numerical Study on the Mechanical Behavior of Composite Steel Structure under Explosion Load. *Materials* **2021**, *14*, 246. [CrossRef] [PubMed]
12. Yin, C.; Jin, Z.; Chen, Y.; Hua, H. Effects of sacrificial coatings on stiffened double cylindrical shells subjected to underwater blasts. *Int. J. Impact Eng.* **2019**, *136*, 103412. [CrossRef]
13. Huang, S.Z.; Tong, X.D. Effects of Internal Fluid on the Dynamic Behaviors of Double Cylindrical Shells Subjected to Underwater Explosion. *J. Offshore Mech. Arct. Eng.* **2022**, *144*, 1–27. [CrossRef]
14. Ning, J.; Meng, F.; Ma, T.; Xu, X. A special numerical method for fluid-structure interaction problems subjected to explosion and impact loading. *Sci. China Technol. Sci.* **2020**, *63*, 1280–1292. [CrossRef]
15. Nassiraei, H.; Yara, A. Local joint flexibility of tubular K-joints reinforced with external plates under IPB loads. *Mar. Struct.* **2022**, *84*, 103199. [CrossRef]
16. Van Vinh, P.; Avcar, M.; Belarbi, M.-O.; Tounsi, A.; Huy, L.Q. A new higher-order mixed four-node quadrilateral finite element for static bending analysis of functionally graded plates. *Structures* **2023**, *47*, 1595–1612. [CrossRef]
17. Van Vinh, P.; Van Chinh, N.; Tounsi, A. Static bending and buckling analysis of bi-directional functionally graded porous plates using an improved first-order shear deformation theory and FEM. *Eur. J. Mech.-A/Solids* **2022**, *96*, 104743. [CrossRef]
18. Zheng, C.; Kong, X.-S.; Wu, W.-G.; Xu, S.-X.; Guan, Z.-W. Experimental and numerical studies on the dynamic response of steel plates subjected to confined blast loading. *Int. J. Impact Eng.* **2018**, *113*, 144–160. [CrossRef]
19. Yao, S.; Zhao, N.; Jiang, Z.; Zhang, D.; Lu, F. Dynamic Response of Steel Box Girder under Internal Blast Loading. *Adv. Civ. Eng.* **2018**, *2018*, 1–12. [CrossRef]
20. Fu, S.; Gao, X.; Chen, X. The similarity law and its verification of cylindrical lattice shell model under internal explosion. *Int. J. Impact Eng.* **2018**, *122*, 38–49. [CrossRef]
21. Wang, H.; Li, Z.; Wu, Y.; Shao, L.; Yao, M.; Liao, Z.; Tang, D. Numerical Simulation Study on Factors Influencing Anti-Explosion Performance of Steel Structure Protective Doors under Chemical Explosion Conditions. *Materials* **2022**, *15*, 3880. [CrossRef]
22. Rajendran, R.; Narashimhan, K.; Narasimhan, K. Performance Evaluation of HSLA Steel Subjected to Underwater Explosion. *J. Mater. Eng. Perform.* **2001**, *10*, 66–74. [CrossRef]
23. Zhong, F.P.; Chen, C.Y.; Lin, J.D. Experimental study of dynamic response of double-walled explosion vessels with flat head. *Explos. Shock Waves* **1999**, *19*, 199–203.
24. Tang, T.G.; Gu, Y.; Li, Q.Z. Expanding fracture of steel cylinder shell by detonation driving. *Explos. Shock Waves* **2003**, *23*, 529–533.
25. Hu, Y.L.; Chen, Z.C.; Wang, W. Non-contact measurement technique for dynamic radial deformation of explosion containment vessels. *J. Mech. Strength* **2009**, *31*, 759–763.
26. Li, J.; Xiong, C.; Zhang, D.Z. Strain Wire Measurement Technique on Process of Circumferential Large Deformation of Cylindrical Explosion Vessels. *Explos. Shock Waves* **2017**, *37*, 976–981.
27. Qin, X.J.; Zhang, D.Z.; Yang, J. Electric probe measurement technique on deformational process of cylindrical steel shell under inside-explosion loading. *Explos. Shock Waves* **2014**, *34*, 115–119.
28. Yang, J.; Wang, K.Y.; Xu, H.B. Development of an optical-fiber displacement interferometer and its application in Hopkinson pressure bar experiment. *Infrared Laser Eng.* **2013**, *42*, 102–107.
29. Deng, J.; Zhou, S.J.; Gao, H.J.; Lin, M.H.; Li, X. Numerical Simulation Investigation on Machining Deformation of AviationThin-Walled Parts Caused by Residual Stress. *Mater. Sci. Forum* **2021**, *1032*, 186–191. [CrossRef]

30. Zhang, D.Z. *Research on Dynamic Load of Cylindrical Explosive Vessel Subjected to Internal Intense Explosion*; Northwest Institute of Nuclear Technology: Xi'an, China, 2012.
31. Sun, C.W.; Wei, Y.Z.; Zhou, Z.K. *Applied Detonation Physics*; Defense Industry Press: Beijing, China, 2000.
32. Zhang, B.P.; Zhang, Q.M.; Huang, F.L. *Detonation Physics*; Arms Industry Press: Beijing, China, 2001.

Disclaimer/Publisher's Note: The statements, opinions and data contained in all publications are solely those of the individual author(s) and contributor(s) and not of MDPI and/or the editor(s). MDPI and/or the editor(s) disclaim responsibility for any injury to people or property resulting from any ideas, methods, instructions or products referred to in the content.